

Interference coordination based on random fractional spectrum reuse in femtocells toward Internet of Things

Guomei Zhang^{1,2} · Man Chu¹ · Jie Li^{1,2}

Received: 1 February 2016 / Accepted: 12 June 2016 / Published online: 25 August 2016
© Springer-Verlag London 2016

Abstract Femtocell is featured with a low-power and low-cost cellular access in indoor environments, and thus offers an effective yet flexible way to implement information exchange over Internet of Things. In femtocell networks, the dense deployment of home eNodeBs causes severe inter-cell interferences and imposes heavier load on the scarce frequency spectrum. In this paper, we propose an inter-femtocell interference coordination scheme to enable random and fractional reuse of frequency resources in a 3D in-building scenario. Specifically, we consider the regular femtocell deployment, where all the femtocells are divided into two groups and two neighboring femtocells will be classified into different group. Each group is initially allocated with a half of frequency resources. To more sufficiently utilize the spectrum, either group of femtocell is allowed to transmit over the frequency assigned to the other group of femtocell in a random way at the cost of introducing some interferences, i.e., reuse based on a specified probability. This probability is determined by maximizing the geometric mean of users' average throughput, such that the fairness among users is guaranteed simultaneously. Moreover, an equivalent scheme generated from full frequency reuse between two femtocells groups is also given. Here, either group of

femtocell will avoid transmitting over fractional frequency randomly with a certain probability and the interference to the adjacent femtocell can be reduced. The simulation results show that the proposed schemes could obtain the larger system average rate and edge user performance compared with the baseline schemes. Moreover, the geometrical average throughput per user achieved by our method is highest, and a more fair resources allocation can be realized.

Keywords Femtocell · Interference coordination · Randomly occupying fractional spectrum · Randomly releasing fractional spectrum · Geometric mean

1 Introduction

Internet of Things can be looked at as a highly dynamic and radically distributed networked system, composed of a very large number of smart objects producing and consuming information. These smart objects can communicate with each other and/or with humans in order to offer a given service, in many cases by wireless connection [1–3]. Under this demand, communications among devices in cellular networks are regarded as the important networking component for Internet of Things (IoT) widely [4]. Many IoT applications occur indoors, including smart homes, smart offices, smart industrial plants and smart museum [5–8]. In these cases, femtocells, which are designed to improve indoor coverage and capacity, can serve as wireless communications devices for the smart objects to access the core network or to correspond with each other.

Femtocells are deployed overlaying the existing macrocells, so the spatial reuse and spectral efficiency can be improved. On one hand, a significant amount of traffic can be moved from the macrocells and the operator's cost can be

✉ Guomei Zhang
zhanggm@mail.xjtu.edu.cn

Man Chu
chumancc@163.com

Jie Li
lijie90@stu.xjtu.edu.cn

¹ School of Electronic and Information Engineering, Xi'an Jiaotong University, Xi'an, China

² Shaanxi Engineering Research Center of Smart Networks and Ubiquitous Access, Xi'an, China

reduced. On the other hand, due to the short transmit distance, the power and battery of user devices can be saved [9]. Thus, femtocell has gained comprehensive attention in recent years. However, with the more cells are introducing into the network, more challenges appears, such as the interference environment becoming more complicated, information security guarantee and QoS provision tending to be more difficult [10–15]. In the two-tier network formed by macrocell and femtocell, there are two kinds of interferences: interference between the macrocell and femtocell, i.e., the cross-tier interference, and the inter-femtocell interference or cotier interference [16, 17].

Early studies mostly focused on the cross-tier interference mitigating. Considering the challenges of the network scale, and the exact number and position of femtocells being unknown by operators, in [18], a distributed dynamic spectrum access and power allocation algorithm are proposed to minimize the sum interference suffered by macrocells' users. In [19, 20], the authors proposed two distributed interference control methods, based on potential game and Q-learning, respectively, to realize a tradeoff between improving the system capacity by introducing the femtocells and compromising the macrocell capacity. Another kind of researches focused on utilizing cognitive radio (CR) channel sensing techniques to determine channel availability and avoid interference to the macrocell users [21–24].

In the above works, it was almost assumed that the number of users in a femtocell is small and the density of the femtocells in a macrocell is low; thus, the inter-femtocell interference had not gained much attention. However, with the progressing of looking for new femtocell markets, the femtocells may be installed in some challenging scenarios, such as the smart apartment buildings and the smart office buildings in IoT, where more femtocells may coexist and numerous users may need to access femtocells. In these scenarios, the interference between the femtocells sharing the same radio resources becomes serious [9]. Therefore, some researchers have addressed the radio resources management problem to coordinate the cotier interference of femtocells in the recent literatures. In view of the on/off states and positions of home eNodeBs (HeNBs) being semi-statically varying, the graph-based dynamic channel allocation methods were proposed to reduce the interference between femtocells [16, 25, 26]. This kind of scheme generally includes three phases: establishment of interference graph, partitioning of femtocells into groups or clusters and allocation of frequency resources among the clusters. Although the graph-based scheme can adapt to the change of the femtocells deployment, the frequency resources cannot be used sufficiently, for the femtocells interfering each other only use the orthogonal channels. Moreover, there is a threshold used in

the interference graph construction, which is difficult to optimize. In addition, the authors of [9] proposed autonomous and coordinated resource allocation algorithms for cotier interference mitigation in femtocell network, over a transmit power minimization-based self-organization rule. Here, the modulation and coding scheme (MCS) of users, subchannels (SCs) and transmit powers (TPs) were jointly assigned in each femtocell. The optimization problem was so difficult to solve that the subproblem of SC and TP allocation is isolated to find a suboptimal solution. In [17], on the basis of taking each femtocell's capacity as the game utility, a distributed subchannel allocation method was designed to coordinate the inter-femtocell interference. In the distributed scheme, the needed information exchange overhead between femtocells is low, but the cost is the decrease in the system performance. Therefore, the centralized interference coordination schemes with reasonable backhaul overhead and complexity are still necessary to obtain a better performance in some scenarios supporting the centralized management, such as an office building, where the base stations (BSs) of femtocells are connected via a wired network to a central controller located within the building [27].

In this paper, we propose an Interference Coordination (IC) method based on reusing partial spectrum randomly for femtocells network, which is built on the orthogonal channel allocation or the full frequency reuse among femtocells, over the assumption of macrocells and femtocells being assigned to orthogonal spectrum. Our major works can be summarized as follows.

- (a) For a regular femtocell block of a multi-story building, all femtocells are divided into two groups based on whether the two femtocells are the direct neighbors. Each group is orthogonally allocated a half of frequency resources initially. In order to improve the frequency using efficiency, we let each femtocell in one group can use the resources of another group randomly with a selected probability in the proportional fairness (PF) user scheduling. This design is called Randomly Occupying Fractional Spectrum (ROFS) scheme.
- (b) For the same scenario, the full frequency resources are initially assigned to both groups of femtocells. Then, in user scheduling, one group of femtocells retreats randomly with a chosen probability over one half of frequency resources. Through the randomly retreating, the interference between the neighboring femtocells could be mitigated. This scheme is named Randomly Releasing Fractional Spectrum (RRFS) scheme.
- (c) To obtain an appropriate probability value, an optimization problem to maximize the geometric

mean of user average throughput is constructed and solved. Here, the geometric mean rather than the arithmetic mean [28] is utilized to guarantee the fairness among users [29, 30], which corresponds with the objective of PF algorithm.

Being similar to the graph-based resources allocation methods, the proposed IC scheme is a kind of dynamic and adaptive channel allocation. But there are some differences between them. First, the applicable scenarios are different. The graph-based frequency allocation method is suitable for the irregular and dynamically changing network topology, which generally includes an adaptive and complicated clustering or grouping process according to the practical inter-femtocell interference level, while our scheme considers a regular femtocell network, so a very simple femtocell grouping scheme is needed. Second, the realization of dynamic resources allocation is different. In the graph-based method, the interference graph is built dynamically, so the final resources allocation can apply to different interference conditions. However, the adaptive frequency allocation is realized through allowing the random fractional spectrum reuse between the femtocells interfering each other in the proposed schemes. Furthermore, the optimized reuse probability according to the practical interference environment makes our schemes adaptable to different interference scenarios.

Moreover, the proposed schemes have two advantages compared with the graph-based ones. Firstly, the higher resource usage efficiency is obtained, for fractional resources would be dynamically and randomly reused between two femtocells interfering each other severely. However, the orthogonal resources are assigned to such femtocells in the graph-based methods, although some users maybe have weak interference and could reuse the same resource. Secondly, there is a threshold in the construction of interference graph, which has important and indirect influence on the performance of graph-based schemes. But it is difficult to optimize this threshold, because the explicit expression between the threshold and the system performance is difficult to build. However, the optimization of the key probability is provided in our schemes.

The remainder of this paper is organized as follows. Section 2 describes the system model, including the femtocells scenario and channel model. The proposed ROFS and RRFS schemes are given in detail in Sect. 3. Section 4 discusses the optimization of the key probability used in ROFS and RRFS. Section 5 presents and analyzes the simulation results. Section 6 summarizes the paper.

2 System model

In this section, the concerned femtocell scenario and the frequency resources structure based on OFDMA are introduced. Then, the channel model is described.

2.1 Femtocell scenario

Let us consider a downlink femtocell network in Fig. 1, where Femto Access Points (FAPs) are densely installed in the apartments of a multi-story building, such as a residence and a commercial building. There is only one stripe of apartments in each floor. Each stripe has M apartments, and the building includes N floors. Each apartment uses one FAP to serve the users in that apartment in a closed access mode, so the total number of FAPs in the network is $N_F = M \times N$. In our study, it is assumed that macrocells and femtocells are allocated to the orthogonal frequency spectrum, so we only focus on the cotier interference of femtocell. In the downlink direction, interference is induced by the transmissions from other FAPs to their served users, as shown by the dashed lines in Fig. 1. In such a regular building, it can be deemed that the strongest interference on one femtocell comes from its neighboring cells, including the cell upstairs, the cell downstairs, the left neighbor and the right neighbor. That is to say the dominant interference links only involve the penetration of one internal wall or floor. This rule will be used in our simple femtocells grouping. It should be noted that, although the interference coordination for downlink communication is mainly studied in this paper, the proposed schemes are also suitable for the uplink one.

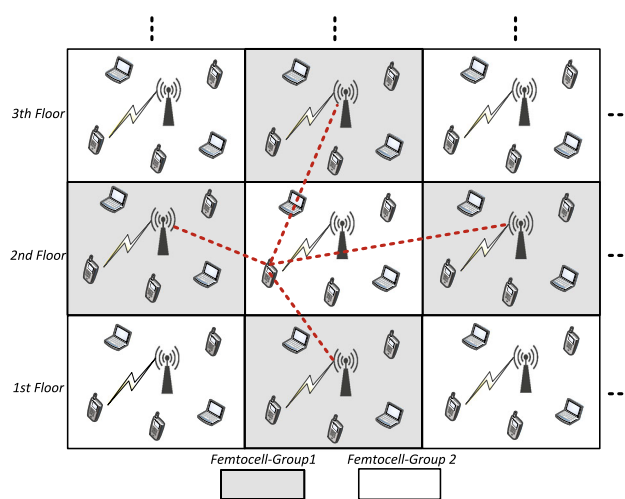


Fig. 1 Illustration of femtocell network

Moreover, in an integrated wired/wireless femtocell scenario given in [27], all the FAPs are connected to a central controller located within the building via a wired network. This central controller may be a femto gateway that could support 20,000 to 500,000 HeNBs per installation [25], and it can be in charge of the optimization of femtocells. Through the femto gateway, the information exchange among femtocells deployed in the same building becomes easy and a centralized interference coordination scheme could be realized.

2.2 Frequency resources structure

LTE radio resource management framework is used in this paper. In LTE system, the downlink multiple access technique is orthogonal frequency division multiple access (OFDMA). The spectrum is divided into resource blocks (RBs), and each RB consists of 12 adjacent subcarriers. For each Transmission Time Interval (TTI), the allocation of RBs will be executed, or the allocating duration is 1 ms [31]. There are a variety of bandwidths supported by LTE, such as 3, 5, 10, 15 and 20 MHz, corresponding to 15, 25, 50, 75 and 100 RBs, respectively. Considering the macrocells would use the major resources, we set the available bandwidth to be 3 MHz on the femtocell tier in the following study.

2.3 Channel model

Because our study focuses on the interference environment among the femtocells deployed in the same building, so an indoor channel model is used which is composed of path loss, shadowing fading and fast fading.

The channel gain in dB on the i -th RB between the user k served by FAP n and FAP m can be expressed as [22, 27]

$$H_{(k,n),m,i} = -PL_{(k,n),m} + \xi_{(k,n),m} + 10\log_{10}(F_{(k,n),m,i}) \quad (1)$$

where the first term represents the propagation loss, and its expression can be written as [32]

$$PL_{(k,n),m} = 38.46 + 20\log_{10}(d_{(k,n),m}) + 0.3d_{(k,n),m} + 18.3a^{((a+2)/(a+1)-0.46)} + qL_{iw}. \quad (2)$$

In Eq. (2), $d_{(k,n),m}$ is the indoor distance in meter between user k in femtocell n and FAP m . a and q are the number of penetrated floors and the number of penetrated walls from user k served by FAP n to FAP m , respectively. L_{iw} is a per wall penetration loss. The first term $38.46 + 20\log_{10}(d_{(k,n),m})$ in (2) is the distance-dependent free space path loss, and the second term $0.3d_{(k,n),m}$ indicates the indoor distance-dependent attenuation modeling the penetration loss of walls within an apartment. The term $18.3a^{((a+2)/(a+1)-0.46)}$ models the propagation loss across

floors, and the last term is the penetration loss of walls between apartments.

The second factor $\xi_{(k,n),m}$ in Eq. (1) represents log-normal shadowing fading with zero mean and a standard deviation of σ_{ξ} . The last term corresponds to Rayleigh fading power in dB between user k of FAP n and FAP m over the i -th RB, with a Rayleigh parameter b meeting $E\{|b|^2\} = 1$. Here, we assume that Rayleigh fading is approximately constant over the subcarriers of a given RB and is independent identically distributed (i.i.d.) over different RBs.

3 Proposed randomly reusing fractional spectrum based IC schemes

This section begins with partitioning the femtocells into groups. According to the positions of femtocells, all the femtocells are divided into two groups as shown in Fig. 1, where one femtocell and its four neighbors are partitioned into different groups. The femtocells indicated by gray filling are classified into group 1, and the femtocells with white filling are partitioned into group 2, denoted by F_1 and F_2 , respectively. Through this grouping, the femtocells in the same group can be regarded as the ones interfering with each other weakly, because the signal transmission from one cell to the other one has to penetrate at least two floors or walls and the signal power decreases quickly. In resource management, we can let them reuse the same frequency spectrum. Assume a same number of users are served in every femtocell, so a same number of frequency resources should be allocated to each group. The number of users per cell is denoted by K . The proposed two interference coordination schemes both obey such a basic resource allocation criterion.

3.1 Randomly occupying fractional spectrum scheme

In order to mitigate the interference of the whole femtocells network, orthogonal frequency resources could be assigned over groups. The total resources are equally partitioned into two parts, one of which is allocated to group 1 and the other one is assigned to group 2. Two resources sets are represented with R_1 and R_2 , respectively.

Considering the users' distribution and channel conditions maybe change in practice, the static resources allocation could not adapt to the variety of interference environment obviously. So the main drawback of orthogonal resources allocation is the low using efficiency of resources. Therefore, we propose a dynamic resources allocation method that allows the femtocells in one group

randomly occupy the resources allocated to another group with a selected probability of p and vice versa. Because how many and which resources of another group would be really occupied by this group in each user scheduling are uncertainty and stochastic, we call this scheme the Randomly Occupying Fractional Spectrum (ROFS)-based interference coordination. The main idea of ROFS scheme is given in Fig. 2. Through selecting an appropriate probability p according to the current interference situation of network, a dynamic frequency reuse can be realized. It should be noted that the similar idea is utilized to coordinate the cross-tier interference in a macro-pico HetNet by us and the performance improvement has been obtained [28]. In this paper, we adjust it to fit for managing cotier interference in femtocells. Moreover, the optimization of probability p is improved to more closely match the PF scheduling algorithm used widely (the detail will be given in Sect. 4).

In user scheduling, one RB can only be allocated to one user in each femtocell at the same time. A full buffer traffic model is assumed for each user, so the resources allocation will go on until all available RBs have been assigned. From Fig. 2, it can be seen that the RBs in R_1 are fixedly allocated to the users in group F_1 . That is to say the RBs in R_1 will be used by the users in F_1 with a probability of 1, while the RBs in R_2 will be used by the users in F_1 with a variable probability p and $0 \leq p \leq 1$. The same case is for F_2 .

The proportional fairness scheduling algorithm is adopted here which can achieve a good balance between overall system throughput and user fairness [29]. In PF scheduling, every user has a scheduling priority over each RB and the one with the highest priority over some RB will be served with this RB. The detail is

$$k_{S,i} = \arg \max_{\{k:Users\}} \{r_{k,i}/\bar{r}_k\}, \tag{3}$$

where $r_{k,i}$ is the user instantaneous data rate at the i -th RB, and \bar{r}_k is the user average data rate counted during a period of time.

In ROFS scheme, the calculation of $r_{k,i}$ has to be adjusted to consider the stochastic interference caused by opposite group that would randomly occupy a fractional

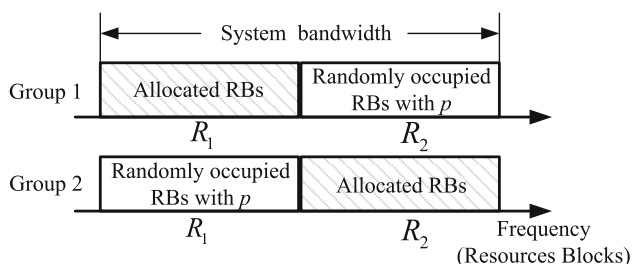


Fig. 2 Schematic of ROFS scheme

spectrum of this group. The modified PF scheduling algorithm is written as

$$\begin{aligned} \text{Case1} : i \in R_1, k_{S,i} &= \arg \max_{\{k \in U_{m_1}\}} \{r_{(k,m_1),i}^{\text{Type1}}(p)/\bar{r}_k\} \\ \text{Case2} : i \in R_2, k_{S,i} &= \arg \max_{\{k \in U_{m_1}\}} \{r_{(k,m_1),i}^{\text{Type2}}(p)/\bar{r}_k\} \\ \text{Case3} : i \in R_2, k_{S,i} &= \arg \max_{\{k \in U_{m_2}\}} \{r_{(k,m_2),i}^{\text{Type1}}(p)/\bar{r}_k\} \\ \text{Case4} : i \in R_1, k_{S,i} &= \arg \max_{\{k \in U_{m_2}\}} \{r_{(k,m_2),i}^{\text{Type2}}(p)/\bar{r}_k\} \end{aligned} \tag{4}$$

In Eq. (4), Case 1 and Case 3 correspond to the case that the users in the femtocells of one group are scheduled at the RBs allocated to the group itself. Case 2 and Case 4 are the cases that the users are scheduled over the RBs of the opposite group. There are two types of instantaneous data rate calculated for different case, and they are both associated with p . In Eq. (4), U_{m_1} and U_{m_2} represent the set of users in the m_1 -th femtocell and the m_2 -th femtocell belonging to F_1 and F_2 , respectively.

When we compute the instantaneous rate, not only the interference from the same group, but also the interference from the other group should be included. For the first type of instantaneous rate, the interference from the other group is dynamic for its randomly occupying behavior. Take Case 1 as an example. Since which femtocell in F_2 would utilize the RBs of R_1 is not known in advance as calculating $r_{(k,m_1),i}^{\text{Type1}}(p)$, it should be averaged over different cases. Then we have

$$r_{(k,m_1),i}^{\text{Type1}}(p) = \sum_{n=0}^{N_2} \left[C_{N_2}^n (1-p)^{N_2-n} p^n E(r_{(k,m_1),i}^n) \right], \tag{5}$$

where

$$E(r_{(k,m_1),i}^n) = \frac{1}{C_{N_2}^n} \sum_{j=1}^{C_{N_2}^n} \left[W_{\text{RB}} \log_2(1 + \text{SINR}_{(k,m_1),i}^{j,n}) \right], \tag{6}$$

$$\begin{aligned} \text{SINR}_{(k,m_1),i}^{j,n} &= \frac{h_{(k,m_1),m_1,i}}{\sum_{b_1 \in F_1, b_1 \neq m_1} \beta_{(k,m_1),b_1} + \sum_{b_2 \in \Xi_{N_2,n,j}} \beta_{(k,m_1),b_2} + \frac{\sigma^2}{P_{\text{RB}}}} \end{aligned} \tag{7}$$

In Eq. (5), $C_{N_2}^n (1-p)^{N_2-n} p^n$ is the probability of the event that the number of femtocells in F_2 using the i -th RB is just n . And the number of the corresponding possible combinations is $C_{N_2}^n$. Furthermore, these possible combinations are written as $\{\Xi_{N_2,n,1}, \dots, \Xi_{N_2,n,C_{N_2}^n}\}$, where the subset $\Xi_{N_2,n,j}$ is the femtocell index set corresponding to the j -th combination, which can be denoted as $\Xi_{N_2,n,j} = \{f_j^1, \dots, f_j^l, \dots, f_j^n\}, \forall f_j^l \in F_2$. In addition, N_l is the size of $F_l (l = 1, 2)$ and W_{RB} is the bandwidth of a RB. P_{RB} is the transmit power at a RB and is assumed to be same

over each RB for every femtocell. σ^2 is noise variance and remains same at each receiver.

Equation (7) gives the instantaneous signal interference and noise ratio (SINR) for one combination $\Xi_{N_2,n,j}$. Here, $h_{\langle k,m_1 \rangle,m_1,i}$ represents the channel fading power from femtocell m_1 to the user k in femtocell m_1 , which can be computed as $h_{\langle k,m_1 \rangle,m_1,i} = 10^{H_{\langle k,m_1 \rangle,m_1,i}/10}$. $\beta_{\langle k,m_1 \rangle,b_1}$ is the large-scale fading power from femtocell b_1 to the user k in femtocell m_1 and can be obtained by $\beta_{\langle k,m_1 \rangle,b_1} = 10^{(-PL_{\langle k,m_1 \rangle,b_1} + \xi_{\langle k,m_1 \rangle,b_1})/10}$. From (7) we can see that only the large-scale fading information is used in calculating the average interference power of denominator. The decoupling of the small-scale fading from the denominator of SINR makes the exchange of cross-channel information among the femtocells only need to follow the change in large scale and the backhaul rate can be reduced significantly. Moreover, the computation complexity could also decrease.

For the second type of instantaneous rate, the interference from the same group is dynamic for its randomly occupying behavior over the other group’s resources. Take Case 2 as an example. For the similar reason to Case 1, $r_{\langle k,m_1 \rangle,i}^{Type2}(p)$ also should be averaged over different cases. Then, we can obtain a group of equations similar to (5)–(7), given by

$$r_{\langle k,m_1 \rangle,i}^{Type2}(p) = \sum_{n=0}^{N_1-1} \left[C_{(N_1-1)}^n (1-p)^{N_1-1-n} p^n E(r_{\langle k,m_1 \rangle,i}^n) \right], \tag{8}$$

$$E(r_{\langle k,m_1 \rangle,i}^n) = \frac{1}{C_{(N_1-1)}^n} \sum_{j=1}^{C_{(N_1-1)}^n} \left[W_{RB} \log_2(1 + \text{SINR}_{\langle k,m_1 \rangle,i}^{j,n}) \right], \tag{9}$$

$$\text{SINR}_{\langle k,m_1 \rangle,i}^{j,n} = \frac{h_{\langle k,m_1 \rangle,m_1,i}}{\sum_{b_1 \in F_2} \beta_{\langle k,m_1 \rangle,b_2} + \sum_{b_1 \in \Xi_{(N_1-1),n,j}} \beta_{\langle k,m_1 \rangle,b_1} + \frac{\sigma^2}{P_{RB}}}. \tag{10}$$

The main difference from Case 1 is that the random interferences come from the other femtocells in the same group excepting the target cell itself.

In Eq. (5), for $p = 0$, only the term corresponding to $n = 0$ has nonzero value, meanwhile, $\Xi_{N_2,0,1}$ is empty. Furthermore, $r_{\langle k,m_1 \rangle,i}^{Type1}(p)$ degenerates into

$$r_{\langle k,m_1 \rangle,i}^{Type1}(0) = \frac{h_{\langle k,m_1 \rangle,m_1,i}}{\sum_{b_1 \in F_1, b_1 \neq m_1} \beta_{\langle k,m_1 \rangle,b_1} + \frac{\sigma^2}{P_{RB}}}, \tag{11}$$

and only the interference from the same group exists. In addition, when the generated random variable x with $x \sim U(0, 1)$ for some RB meets $x < p$, the Case 2 or Case 4

would be just involved. That is to say the Case 2 and Case 4 would be deleted for $p = 0$ because the condition $x < p$ will never be met. Thus, when $p = 0$, the ROFS scheme will degenerate into the orthogonal channel allocation.

On the other hand, only the terms corresponding to $n = N_2$ in (5) and $n = N_1 - 1$ in (8) have nonzero values for $p = 1$, meanwhile, $\Xi_{N_2,N_2,1} = F_2$ and $\Xi_{(N_1-1),N_1,1} = F_1 \setminus m_1$. Thus, we achieve

$$r_{\langle k,m_1 \rangle,i}^{Type1}(1) = r_{\langle k,m_1 \rangle,i}^{Type2}(1) = \frac{h_{\langle k,m_1 \rangle,m_1,i}}{\sum_{b_1 \in F_1, b_1 \neq m_1} \beta_{\langle k,m_1 \rangle,b_1} + \sum_{b_2 \in F_2} \beta_{\langle k,m_1 \rangle,b_2} + \frac{\sigma^2}{P_{RB}}} \tag{12}$$

and all femtocells excepting the serving one would generate the interference to the target user. In this case, the ROFS scheme becomes the full frequency reuse. That is to say the traditional orthogonal frequency allocation and full frequency reuse are the special cases of the ROFS scheme.

To describe clearly, the procedure of ROFS is given in detail as follows:

Input: p , the optimized probability calculated and informed by the central controller.

Output: The scheduling results of the t -th TTI, i.e. $\{k_{S,i}^{m_l} \mid k_{S,i}^{m_l} \in U_{m_l}, m_l \in F_l (l = 1, 2), i \in R_1 \cup R_2\}$.

Initialization: $\{\bar{r}_{\langle k,m_l \rangle} = \bar{r}_{\langle k,m_l \rangle}^{(t-1)}, m_l \in F_l, \forall k \in U_{m_l}\} (l = 1, 2)$

for $l = 1 : 2$ **do**

for $m_l = F_l(1) : F_l(N_l)$ **do**

for $i = R_l(1) : R_l(\text{size}(R_l))$ **do**

$k_{S,i}^{m_l} = \arg \max \frac{r_{\langle k,m_l \rangle,i}^{Type1}(p)}{\bar{r}_{\langle k,m_l \rangle}}, k \in U_{m_l};$

$\bar{r}_{\langle k_{S,i}^{m_l}, m_l \rangle} = \bar{r}_{\langle k_{S,i}^{m_l}, m_l \rangle} + r_{\langle k_{S,i}^{m_l}, m_l \rangle,i}^{Type1}(p);$

end for

for $i = R_{\{1,2\} \setminus l}(1) : R_{\{1,2\} \setminus l}(\text{size}(R_{\{1,2\} \setminus l}))$ **do**

$x = \text{rand};$

if $x < p$

$k_{S,i}^{m_l} = \arg \max \frac{r_{\langle k,m_l \rangle,i}^{Type2}(p)}{\bar{r}_{\langle k,m_l \rangle}}, k \in U_{m_l};$

$\bar{r}_{\langle k_{S,i}^{m_l}, m_l \rangle} = \bar{r}_{\langle k_{S,i}^{m_l}, m_l \rangle} + r_{\langle k_{S,i}^{m_l}, m_l \rangle,i}^{Type2}(p)$

end if

end for

end for

end for

Update: $\{\bar{r}_{\langle k,m_l \rangle}^t = \bar{r}_{\langle k,m_l \rangle}, \forall m_l \in F_l, \forall k \in U_{m_l}\}$.

3.2 Randomly releasing fractional spectrum scheme

In order to maximize the using efficiency of resources, full frequency reuse among femtocells in the network can be

adopted. However, the interference is very severe in such case. To mitigate the interference, a dynamic resources allocation method, called Randomly Releasing Fractional Spectrum (RRFS) scheme, is presented that allows the femtocells randomly releasing partial resources allocated to them with a selected probability of p . The basic idea of RRFS is shown in by Fig. 3.

Full system bandwidth is assigned to all the femtocells in network initially, while in user scheduling, the RBs in the set R_2 will be released with an optimized probability p by each femtocell in group 1 and group 2 would retreat over the set R_1 with the same probability.

The modified PF scheduling algorithm for RRFS still can be written as Eq. (4). The change takes place in the calculation of the instantaneous SINR in Eqs. (7) and (10). They are revised to the following forms:

$$\text{SINR}_{(k,m_1),i}^{j,n} = \frac{h_{(k,m_1),m_1,i}}{\sum_{b_1 \in F_1, b_1 \neq m_1} \beta_{(k,m_1),b_1} + \sum_{b_2 \in \Omega_{N_2,n,j}} \beta_{(k,m_1),b_2} + \frac{\sigma^2}{P_{\text{RB}}}}, \tag{13}$$

$$\text{SINR}_{(k,m_1),i}^{j,n} = \frac{h_{(k,m_1),m_1,i}}{\sum_{b_2 \in F_2} \beta_{(k,m_1),b_2} + \sum_{b_1 \in \Omega_{(N_1-1),n,j}} \beta_{(k,m_1),b_1} + \frac{\sigma^2}{P_{\text{RB}}}}, \tag{14}$$

where the subsets $\Omega_{N_2,n,j}$ and $\Omega_{(N_1-1),n,j}$ are the complementary sets of $\Xi_{N_2,n,j}$ and $\Xi_{(N_1-1),n,j}$, i.e., $\Omega_{N_2,n,j} = F_2 \setminus \Xi_{N_2,n,j}$ and $\Omega_{(N_1-1),n,j} = F_1 \setminus \Xi_{(N_1-1),n,j}$. Because the selected n femtocells from the set F_2 and F_1 will not use the target RB in RRFS scenario, the interference must come from the rest of femtocells.

In fact, the RRFS scheme with p can be seen as the ROFS scenario with $(1 - p)$. The two schemes are equivalent completely. Under the same network topology and channel conditions, the optimized two probabilities must be complementary with each other in the case of the optimization objective being same.

3.3 Complexity and memory usage analysis

Compared with the traditional PF scheduler, the computation overhead of ROFS scheme increases for the

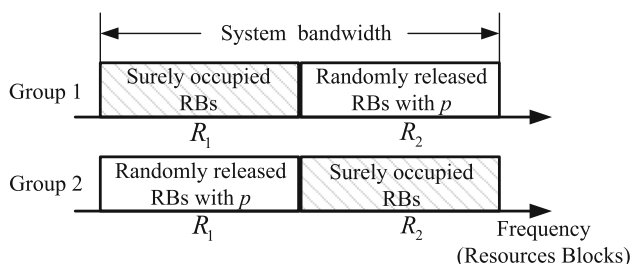


Fig. 3 Schematic of RRFS scheme

computation of average instantaneous throughput in (5) and (8). Since the average interference powers depending on the large-scale fading is used in Eqs. (7) and (10), they could be calculated preceding the scheduling. So this part of complexity can be ignored from the view of the small scale. The additional computation cost of our schemes is caused by calculating $r_{(k,m_1),i}^{\text{Type1}}(p)$ and $r_{(k,m_1),i}^{\text{Type2}}(p)$, which will be averaged over $\sum_{n=0}^{N_2} C_{N_2}^n$ and $\sum_{n=0}^{N_1-1} C_{N_1-1}^n$ cases for Case 1 and Case 2 in (4), respectively. Moreover, only when the condition $x < p$ is met, $r_{(k,m_1),i}^{\text{Type2}}(p)$ needs to be calculated for each RB in $R_{\{1,2\} \setminus i}$. Therefore, the ROFS scheme increases the complexity by about $(2^{N_1} + 2^{N_2})(4 + pN_{\text{RB}})/8$ (Here, N_{RB} is the size of $R_1 \cup R_2$) times for calculating the user scheduling priority against the orthogonal resources allocation. If the instantaneous interference power related with the small-scale fading is utilized, the complexity will be increased by about $(1 + pN_{\text{RB}})(N_1 + N_2)/2 + [N_2 + pN_{\text{RB}}(N_2 - 1)/4]2^{N_2-2} + [N_1 + pN_{\text{RB}}(N_1 - 1)/4]2^{N_1-2}$ times.

The average interference powers involved in Eqs. (7) and (10) are recalculated when the large-scale fading coefficients change. Subsequently, these data should be saved by each FAP to be ready for calculating $r_{(k,m_1),i}^{\text{Type1}}(p)$ and $r_{(k,m_1),i}^{\text{Type2}}(p)$ in each scheduling slot. Assume each power value is represented by four bytes, then the required memory for storing these average interference powers is about $3(2^{N_1} + 2^{N_2})$ bytes.

Obviously, the computation complexity and the memory usage have significant improvement for a large-scale femtocell network. Through reducing interference femto-cells set of the target cell, the complexity and storage space needed could decrease evidently.

4 Optimization of the probability in ROFS and RRFS schemes

4.1 Problem formulation

In the proposed ROFS and RRFS schemes, a key parameter is the probability p . An appropriate p can achieve a relative good tradeoff between the frequency using efficiency and interference mitigation. It is obvious that the probability p should be dynamically selected according to the networks topology and channel conditions. Because the user scheduling is executed for each TTI, a precise modification of p should be able to follow the fast fading channel information. However, this will lead to a high computation cost for the central controller as well as a huge backhaul overhead for the network. Then, we choose to optimize the

probability p from a long-term view and only utilize the global large-scale channel information.

In [28], we took the arithmetic mean of user throughput as the optimization objective for the probability p . That is equivalent to maximizing the system sum rate. A reasonable resources distribution algorithm should consider the fairness among users and can improve both cell edge user throughput and sum user throughput. For this target, the PF user scheduling is used in ROFS and RRFS schemes. Therefore, the geometric mean of user throughput is introduced to optimize p . The corresponding objective can be set to maximize $\sum_{k \in U} \log(r_k)$ [30], where r_k is the throughput of user k .

The optimization of p in both ROFS and RRFS schemes is same, so the ROFS is taken as an example here. In ROFS scenario, two parts of RBs are both used by all the femtocells of the network. From the view of one part of RBs set R_1 , the aggregate utility function based on the geometric mean of user throughput can be written as

$$O_{R_1}(p) = \sum_{m_1 \in F_1} \sum_{k \in U_{m_1}} \log\left(\frac{1}{K} \tilde{r}_{(k,m_1)}^{\text{Type1}}(p)\right) + \sum_{m_2 \in F_2} \sum_{k \in U_{m_2}} \log\left(\frac{1}{K} p \tilde{r}_{(k,m_2)}^{\text{Type2}}(p)\right) \quad (15)$$

where

$$\tilde{r}_{(k,m_1)}^{\text{Type1}}(p) = \sum_{n=0}^{N_2} \left[C_{N_2}^n (1-p)^{N_2-n} p^n E(\tilde{r}_{(k,m_1)}^n) \right], \quad (16)$$

$$E(\tilde{r}_{(k,m_1)}^n) = \frac{1}{C_{N_2}^n} \sum_{j=1}^{C_{N_2}^n} \left[N_{\text{RB}}^{R_1} W_{\text{RB}} \log_2(1 + \text{SINR}_{(k,m_1)}^{j,n}) \right], \quad (17)$$

$$\text{SINR}_{(k,m_1)}^{j,n} = \frac{\beta_{(k,m_1),m_1}}{\sum_{b_1 \in F_1, b_1 \neq m_1} \beta_{(k,m_1),b_1} + \sum_{b_2 \in \Xi_{N_2,n,j}} \beta_{(k,m_1),b_2} + \frac{\sigma^2}{P_{\text{RB}}}} \quad (18)$$

$$\tilde{r}_{(k,m_2)}^{\text{Type2}}(p) = \sum_{n=0}^{N_2-1} \left[C_{(N_2-1)}^n (1-p)^{N_2-1-n} p^n E(\tilde{r}_{(k,m_2)}^n) \right], \quad (19)$$

$$E(\tilde{r}_{(k,m_2)}^n) = \frac{1}{C_{(N_2-1)}^n} \sum_{j=1}^{C_{(N_2-1)}^n} \left[N_{\text{RB}}^{R_1} W_{\text{RB}} \log_2(1 + \text{SINR}_{(k,m_2)}^{j,n}) \right], \quad (20)$$

$$\text{SINR}_{(k,m_2)}^{j,n} = \frac{\beta_{(k,m_1),m_1}}{\sum_{b_1 \in F_2} \beta_{(k,m_1),b_2} + \sum_{b_1 \in \Xi_{(N_1-1),n,j}} \beta_{(k,m_1),b_1} + \frac{\sigma^2}{P_{\text{RB}}}} \quad (21)$$

The first term in (15) corresponds to the performance metric of users in the set F_1 over R_1 and the second term is the metric of users in the set F_2 over R_1 . Different from $r_{(k,m_1),i}^{\text{Type1}}(p)$ and $r_{(k,m_2),i}^{\text{Type2}}(p)$ in Eq. (4), the $\tilde{r}_{(k,m_1)}^{\text{Type1}}(p)$ and $\tilde{r}_{(k,m_2)}^{\text{Type2}}(p)$ here are only related to the large-scale channel information. Due to the large-scale fading being same on every RB for a certain user, the average throughput of this user over R_1 would be $N_{\text{RB}}^{R_1}$ times of the average rate on one RB, where $N_{\text{RB}}^{R_1}$ is the number of RBs in the set R_1 . On the other hand, although the scheduling results depends on the fast fading information in PF scheduling, each user still has equal opportunity to be scheduled from the view of long term [29]. There are K users sharing the RBs set R_1 in a femtocell, so each user could use $1/K$ resources in R_1 averagely. That is why a coefficient of $1/K$ exists before $\tilde{r}_{(k,m_1)}^{\text{Type1}}(p)$ and $\tilde{r}_{(k,m_2)}^{\text{Type2}}(p)$ in (15).

In the same way, the aggregate utility function for R_2 has the expression of

$$O_{R_2}(p) = \sum_{m_1 \in F_1} \sum_{k \in U_{m_1}} \log\left(\frac{1}{K} p \tilde{r}_{(k,m_1)}^{\text{Type2}}(p)\right) + \sum_{m_2 \in F_2} \sum_{k \in U_{m_2}} \log\left(\frac{1}{K} \tilde{r}_{(k,m_2)}^{\text{Type1}}(p)\right). \quad (22)$$

At last, we establish the optimization problem for the probability p given by

$$\max_{0 < p < 1} O(p) = [O_{R_1}(p) + O_{R_2}(p)]. \quad (23)$$

Here, for $p = 0$, we have

$$O(0) = \sum_{m_1 \in F_1} \sum_{k \in U_{m_1}} \log\left(\frac{1}{K} R_{(k,m_1)}^{\text{Type1}}(0)\right) + \sum_{m_2 \in F_2} \sum_{k \in U_{m_2}} \log\left(\frac{1}{K} R_{(k,m_2)}^{\text{Type1}}(0)\right). \quad (24)$$

The optimized p^* achieved through solving (23) would be compared with the two end points $p = 0$ and $p = 1$. The one with the maximal $O(p)$ would be selected.

4.2 Problem solving

The target function in (23) has the form of the sum of logarithmic function. If the subfunctions $\tilde{r}_{(k,m_1)}^{\text{Type1}}(p)$ and $p \tilde{r}_{(k,m_2)}^{\text{Type2}}(p)$ within the brackets of logarithmic function are concave in the range of $0 < p < 1$, the whole target function will be concave. From Eqs. (16) and (19), we can see that they are the sum of high-order polynomials. Take $\tilde{r}_{(k,m_1)}^{\text{Type1}}(p)$

for example. We should testify whether each term $r_{(k,m_1)}^{N_2,n}(p) = C_{N_2}^n (1-p)^{N_2-n} p^n E(\tilde{r}_{(k,m_1)}^n)$ in the summation is concave. According to the definition of a concave function, if its second derivative is less than zero over a target range, it will be concave. The second-order derivative of $r_{(k,m_1)}^{N_2,n}(p)$ with respect to p is

$$r_{(k,m_1)}^{nN_2,n}(p) = C_{N_2}^n E(\tilde{r}_{(k,m_1)}^n) [(n - N_2 p)^2 p^{-2} (1-p)^{-2} - np^{-2} - (N_2 - n)(1-p)^{-2}] (1-p)^{N_2-n} p^n. \tag{25}$$

Unfortunately, we could not prove that $r_{(k,m_1)}^{nN_2,n}(p)$ is less than zero in $0 < p < 1$ for each n . For example, $r_{(k,m_1)}^{nN_2,0}(p) = E(\tilde{r}_{(k,m_1)}^0) N_2(N_2 - 1)(1-p)^{N_2-2} > 0$ for a relatively large N_2 , while $r_{(k,m_1)}^{nN_2,N_2}(p) = E(\tilde{r}_{(k,m_1)}^{N_2}) N_2(N_2 - 1)(1-p)^{N_2-2} > 0$. In addition, for $n = 1$, we obtain that $r_{(k,m_1)}^{nN_2,1}(p) = N_2 E(\tilde{r}_{(k,m_1)}^1) (N_2 p - 2)(N_2 - 1)(1-p)^{N_2-3} > 0$ with $p > 2/N_2$ and $r_{(k,m_1)}^{nN_2,1}(p) < 0$ with $p < 2/N_2$. From the above analysis, we can see that it is difficult to ascertain the problem of (23) being concave or convex, especially it is still related to the network topology and channel conditions. Furthermore, we cannot use the cvx tool box to solve (23).

Moreover, the first-order derivative of $O(p)$ with respect to p has a form of the sum of high-order rational fraction. It is also difficult to solve the problem (23) through finding the zero-crossing positions of the first-order derivative of $O(p)$.

However, the optimization variable p is only a scalar in the range of $0 \leq p \leq 1$ fortunately. We can perform an exhaustive search to find a suboptimal p over a discrete set $[0 : \Delta : 1]$. In such case, the step length Δ will determine the complexity and precision of the search.

In addition, the other suboptimal approaches such as particle swarm optimization (PSO) algorithm in [33] can also be applied. The PSO-based optimization algorithm for problem (23) is described as the following procedure:

Step 1 Initialize the velocity and location of particles according to the constraint of p . The velocity and location of the j -th particle of p as

$$v_p^j(1) = \varepsilon - 1/2, \quad p^j(0) = 1/2, \tag{26}$$

where $\varepsilon \in U(0, 1)$ and $j = 1, 2, \dots, S$ is the index of the particle. S denotes the number of the particles in a swarm.

Step 2

- (a) Update the velocity and location of each particle according to the PSO update formulas [33]:

$$\begin{cases} v_p^j(\tau) = av_p^j(\tau - 1) + c_1 b_1 [O_p^j(\tau - 1) - p^j(\tau - 1)] \\ \quad \quad \quad + c_2 b_2 [O_p^g(\tau - 1) - p^g(\tau - 1)] \\ p^j(\tau) = p^j(\tau - 1) + v_p^j(\tau), \end{cases} \tag{27}$$

where b_1 and b_2 are random numbers following the uniform distribution between 0 and 1. c_1 and c_2 are the learning factors and have to meet $0 < c_1 + c_2 < 4(1 + a)$ to ensure the convergence of the PSO algorithm. a is the inertia factor and set as $a = 1.2 - 0.4\tau/T_{\max}$ in the simulation, where τ is the index of iteration and T_{\max} is the maximum number of iterations. O_p^j is the local optimum position of particles and O_p^g is the global optimum position of particles. p^j and v_p^j are the position and velocity of j -th particle, respectively.

- (b) Judge whether $p^j(\tau)$ is within its range. If it exceeds the range, let $v_p^j(\tau) = v_p^j(\tau)/2$ and then update $p^j(\tau)$ again.
- (c) Set $O(p)$ to be the fitness function. Then compare the values of all fitness functions obtained from previous iterations and achieve the local optimum values $O_p^j(\tau)$ and the global optimum value $O_p^g(\tau)$.
- (d) If the maximal iteration is reached or $[O_p^g(\tau) - O_p^g(\tau - 1)] < \delta$, where δ is a small constant, the iteration is stopped. Otherwise, set $\tau = \tau + 1$ and go to step (b).

4.3 Complexity analysis

The main computation overhead for the optimization of p includes two aspects: (1) Calculation of the average throughput $E(\tilde{r}_{(k,m_1)}^n)$ and $E(\tilde{r}_{(k,m_2)}^n)$ in Eqs. (16) and (19), which are independent to the variable p and can be calculated before solving the optimization problem. Considering the dominant multiply operations, the computation complexity of calculating the average throughput is $C_1 = K(N_1 + N_2)(N_2 2^{N_2} + N_1 2^{N_1}) + K(N_1 + N_2)^2$. (2) Performing the PSO algorithm to find the suboptimal p . This operation’s computation complexity is $C_2 = K[N_2^2 N_1 + (N_2 - 1)^2 N_2 + N_1^2 N_2 + (N_1 - 1)^2 N_1]ST$, where T represents the realistic number of iterations. Only when the large-scale fading information changes, the above operations have to be per-

formed by the central controller of network. Therefore, the computing cost is reasonable and acceptable.

4.4 Implementation steps of ROFS and RRFS schemes in femtocell network

From the previous description, it can be seen that the proposed IC scheme includes two main implementation phases, namely the optimization of the probability p and the PF scheduling. For an integrated wired/wireless femtocell network having a central controller, a centralized IC method is applicable. The implementation steps of the proposed IC scheme in a centralized form are as follows: First, all the FAPs sent the large-scale channel information of users collected to the central controller; then, the central controller calculates the optimized probability p by using the optimization method given above in this section. Furthermore, the average interference powers correlated with the long time channel information that are used in Eqs. (7) and (10) are calculated and saved by each FAP simultaneously. Subsequently, the central controller transmits p to each FAP. During this phase, there is signaling interaction over the wired links. However, the needed backhaul overhead is not too high, for the signaling interaction only occurs when the long time channel information changes. Second, all FAPs allocate the RBs to their users according to Eq. (4) in each scheduling slot based on the information saved in memory or received from the central control node previously.

5 Simulation evaluations

5.1 Simulation settings

In this section, simulation results are presented to evaluate the proposed ROFS and RRFS schemes. They will be compared with full frequency reuse (FR) and fractional FR.

Table 1 Simulation parameters in femtocell network

Parameters	Assumptions
Bandwidth	3 MHz
Number of RBs	16
Number of apartment	$4 \times 4, 3 \times 3$
Size of apartment	$10 \times 10 \times 3$ ($L \times W \times H$)
Number of users per cell	6
User distribution	Uniformly and randomly
Traffic model	Full buffer
Standard deviation of shadowing	8 dB
Penetration loss per wall	5 dB
Noise power density	-174 dBm/Hz

The 3D femtocells deployment scenario described in Sect. 2 is assumed and modeled. Here, only one femtocell block shown in Fig. 1 is considered. Detailed simulation parameters are listed in Table 1.

5.2 Simulation for the optimization of p

Figure 4 plots the utility function in the optimization of p for ROFS and RRFS schemes under three users' distribution scenarios. Each curve corresponds to one user drop selected from three users' location cases. The number of femtocells is 4×4 , and there are 6 users in every femtocell. The found points through solving the optimization problem of (23) are also marked. As shown in Fig. 4a, b, the optimization method given in Sect. 4 can accurately find the maximal value point of the utility function in our optimization problem. In addition, for the scene of users distributing close to the serving FAP, it is preferable that more resources are reused over two femtocells group, i.e., a larger p for ROFS and a smaller p for RRFS. When the users concentrate upon the femtocell's edge, a lower resource reuse factor is better. These results agree with our general knowledge and demonstrate the designed optimization method is reasonable and available. Moreover, we can see that the optimized p for ROFS approximately equals the result of subtracting the optimized p of RRFS from 1. (Because the user drops for two subfigures are different, so the two probabilities for the same user distribution case have not strict complementary relationship). This result corresponds with the analysis in Sect. 3.2 of Sect. 3.

5.3 Simulation results for different schemes

In order to reduce the backhaul overhead and the computation complexity, only the large-scale fading information is adopted in calculating the interference power of instantaneous SINR in our IC schemes. Figure 5 exhibits the performance loss induced by this simplified process in ROFS method with the same scenario as shown in Fig. 4. We can see that there is about 9 % loss of user rate at 50 % point. But the benefit is that the backhaul cost could decrease about $N_F * N_T$ times and the computation complexity declines for near $N_F/2$ times, where N_F and N_T are the number of femtocells of network and the number of TTIs in simulation, respectively. In our simulation, we assume the channel changes independently over different TTIs, but the realistic channel may change more slowly for the devices indoor usually move in a low speed or remain static. In this case, the performance loss caused by prohibiting small-scale fading information would mitigate further.

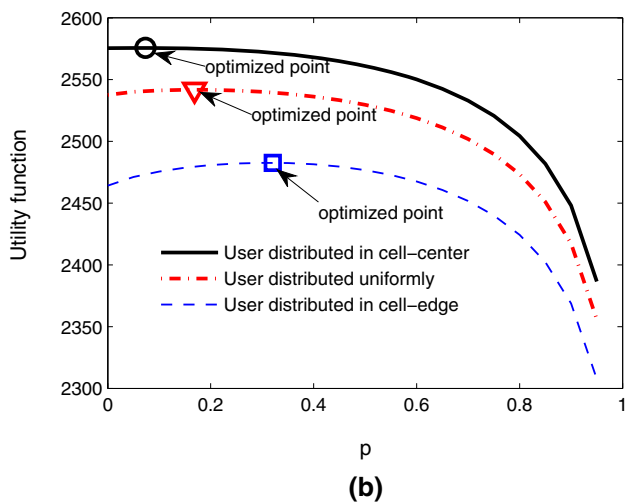
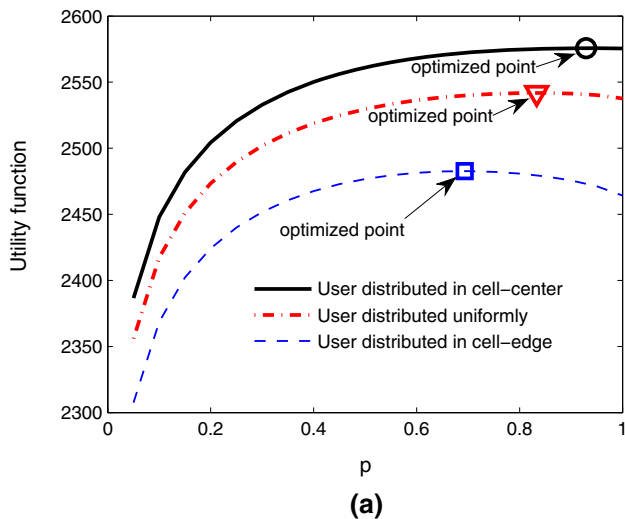


Fig. 4 Utility function versus variable p and the optimization result in the proposed schemes. **a** ROFS scheme. **b** RRFS scheme

Figure 6 depicts the Cumulative Distribution Function (CDF) curves of the user average throughput for four schemes. The simulation scenario is still that of 4×4 cells and 6 users per cell. Moreover, in fractional FR scene, edge users are assumed to be $1/4$ of the total users. It can be seen that the ROFS and RRFS methods have the same performances. The analysis result in Sect. 3 is verified that the ROFS and RRFS methods are completely equivalent. In addition, our schemes have better edge user performance than full FR and higher system average performance than fractional FR. In fractional FR scene, the edge users would utilize orthogonal spectrum between two neighboring femtocells, so a better edge performance can be obtained. From Fig. 6, we can see that the proposed scheme has similar edge user rate with fractional FR at the cost of a certain system average performance loss against full FR.

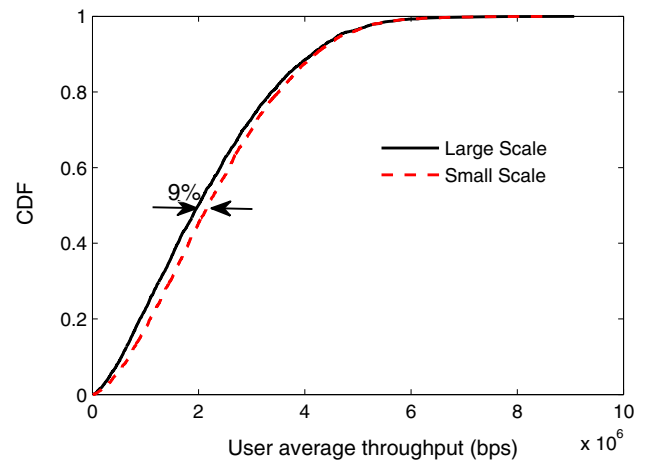


Fig. 5 Performance comparison of two cases that interference powers are calculated by using the large-scale fading information and the small-scale fading information

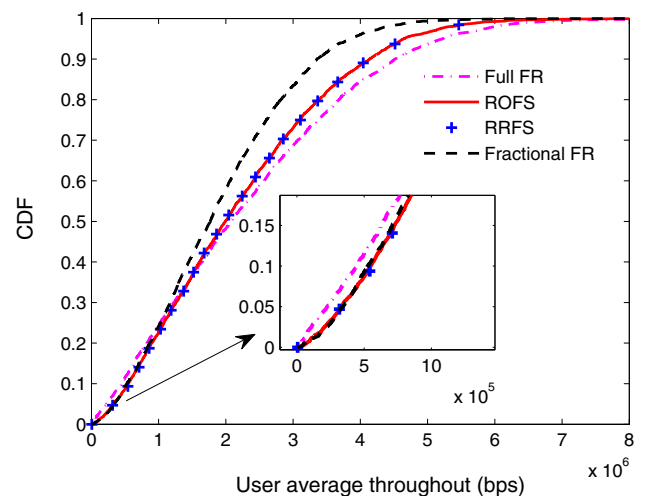


Fig. 6 User throughput CDF curves

The arithmetic average throughput of user is given in Fig. 7 for 3×3 and 4×4 femtocells network. Since the interference environment in 3×3 scene is better than 4×4 network, so the performance of the former scenario is higher for all the IC schemes. Moreover, we can see that the proposed methods have about 13.7 % improvement and 5.2 % loss in terms of user arithmetic average throughput relative to fractional FR and full FR in 3×3 scenario, respectively. In the 4×4 network, these two proportions become to 16.5 and 5.6 %. That is to say the performance gain of our method over the fractional FR is more obvious with the interference tending to be more serious.

In Fig. 8, the geometrical average throughput of user is depicted. It can be seen that the proposed methods are best in terms of geometrical average rate. Therefore, our

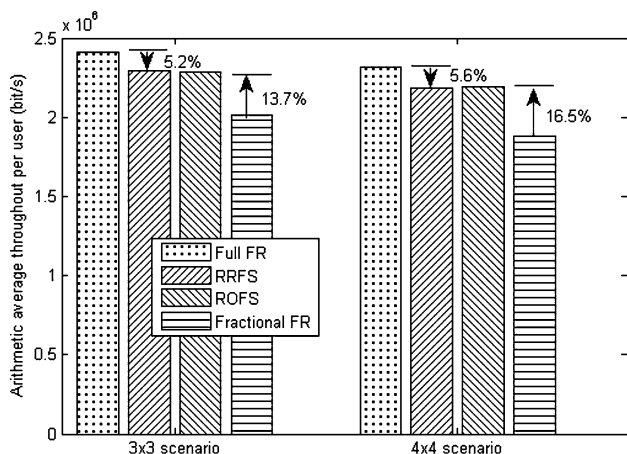


Fig. 7 Arithmetic average throughput of user

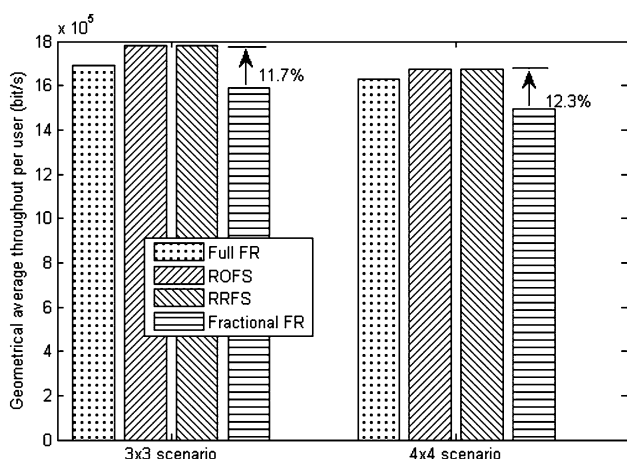


Fig. 8 Geometrical average throughput of user

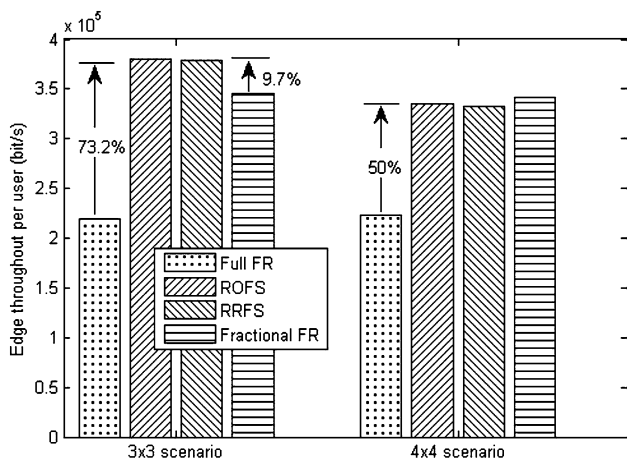


Fig. 9 Edge user throughput

methods can more effectively guarantee the fairness of users among all schemes. This result consists with the optimization target in Sect. 4.

The edge user throughput, i.e., the performance of 5 % users in CDF curve, is shown in Fig. 9. The edge user rate of the proposed schemes is improved by 73.9 and 50 % compared with full FR in 3×3 and 4×4 scenario. For 3×3 scene with lighter interference, the edge user performance is even better than fractional FR. With the inter-femtocell interference becoming more severe, the edge user rate of our methods would decrease and may be lower than fractional FR. That is because edge users are not isolated to orthogonally allocate resources as done in fractional FR and the total user average performance is the design objective in the proposed schemes.

6 Conclusions

A kind of dynamically changing frequency reuse factor-based IC scheme is proposed for femtocell network in this paper. Here, a probability p , with which one femtocell group randomly occupies or releases fractional frequency resources, is introduced and optimized to realize the tradeoff between mitigating inter-femtocell interference and improving the usage efficiency of spectrum. Compared with fractional FR used widely in macrocell network, the proposed schemes can achieve higher arithmetic average user throughput. Moreover, a better edge user performance is got by our methods relative to full frequency reuse. In addition, the new methods can obtain the maximal geometrical average user’ rate compared with the other schemes and realize more fairly allocation of resources among users. What’s more, in current ROFS and RRFS schemes, only one p is used and designed for all the users in each femtocell from the view of average performance of network. However, the preferable p for different user location is distinct, just as shown in Fig. 4. Therefore, a more precise design should use different p for users located in different areas of a cell, such as cell center and cell edge. This will be focused on in our following work.

Acknowledgments This work is supported by National Natural Science Foundation of China (NSFC) under Grant No. 61461136001 and the Fundamental Research Funds for the Central Universities of China.

References

- Miorandi D, Sicari S, Pellegrini FD et al (2012) Internet of things: vision, applications and research challenges. *Ad Hoc Netw* 10(7):1497–1516
- Yunchuan S, Antonio J (2014) An extensible and active semantic model of information organizing for the internet of things. *Pers Ubiquit Comput* 18(8):1821–1833
- Sun Y, Yan H, Zhang J, Xia Y, Wang S, Bie R, Tian Y (2014) Organizing and querying the big sensing data with event-linked network in the internet of things. *Int J Distrib Sens Netw* 2014:1–11

4. Qinghe Du, Song Houbing, Qian Xu, Ren Pinyi, Sun Li (2015) Interference-controlled D2D routing aided by knowledge extraction at cellular infrastructure towards ubiquitous CPS. *Pers Ubiquit Comput* 19(7):1033–1043
5. Atzori L, Iera A, Morabito G (2010) The internet of things: a survey. *Comput Netw* 54(15):2787–2805
6. Yunchuan S, Hongli Y, Cheng L, Rongfang B, Zhangbing Z (2014) Constructing the web of events from raw data in the web of things. *Mob Inf Syst* 10(1):105–125
7. Su Z, Xu Q, Zhu H, Wang Y (2015) A novel design for content delivery over software defined mobile social networks. *IEEE Netw* 29(4):62–67
8. Su Z, Xu Q, Qi Q (2016) Big data in mobile social networks: a QoE oriented framework. *IEEE Netw* 30(1):52–57
9. Lopez-Perez D, Chu X, Vasilakos AV et al (2014) Power minimization based resource allocation for interference mitigation in OFDMA femtocell networks. *IEEE J Sel Areas Commun* 32(2):333–344
10. Sun Y, Bie R, Zhang J (2016) Measuring semantic-based structural similarity in multi-relational networks. *Int J Data Warehous Min* 12(1):20–33
11. Mukhtar H, Qinghe D, Li S, Pinyi R (2016) Security enhancement for video transmission via noise aggregation in immersive systems. *Multimed Tools Appl* 75(9):5345–5357
12. Du Q, Xi Z (2010) Statistical QoS provisionings for wireless unicast/multicast of multi-layer video streams. *IEEE J Sel Areas Commun* 28(3):420–433
13. Ge X, Yang B, Ye J, Mao G, Wang C, Han T (2015) Spatial spectrum and energy efficiency of random cellular networks. *IEEE Trans Commun* 63(3):1019–1030
14. Qinghe D, Weidong Z, Weimin L, Xuelin Z, Bo S, Houbing S, Pinyi R, Li S, Yichen W (2016) Massive access control aided by knowledge-extraction for co-existing periodic and random services over wireless clinical networks. *J Med Syst* 40:171
15. Li S, Pinyi R, Qinghe D, Yichen W (2016) Fountain-coding aided strategy for secure cooperative transmission in industrial wireless sensor networks. *IEEE Trans Ind Inf* 12(1):291–300
16. Zheng K, Wang Y, Lin C et al (2011) Graph-based interference coordination scheme in orthogonal frequency-division multiplexing access femtocell networks. *IET Commun* 5(17):2533–2541
17. Xu C, Sheng M, Wang X et al (2014) Distributed subchannel allocation for interference mitigation in OFDMA femtocells: a utility-based learning approach. *IEEE Trans Veh Technol* 64(6):1–1
18. Su Q, Huang A, Wu Z, et al (2009) A distributed dynamic spectrum access and power allocation algorithm for Femtocell networks. In: international conference on wireless communications and signal processing, pp 1–5
19. Giupponi L, Ibars C (2010) Distributed interference control in OFDMA-based femtocells. In: 2010 IEEE 21st international symposium on personal indoor and mobile radio communications (PIMRC), pp 1201–1206
20. Galindo-Serrano A, Giupponi L (2010) Distributed Q-learning for interference control in OFDMA-based femtocell networks. In: IEEE vehicular technology conference, pp 1–5
21. Lien SY, Lin YY, Chen KC (2011) Cognitive and game-theoretical radio resource management for autonomous femtocells with QoS guarantees. *IEEE Trans Wirel Commun* 10(7):2196–2206
22. Yaacoub E (2015) Interference mitigation in femtocell networks with joint channel sensing and resource allocation. In: Wireless communications and networking conference (WCNC), pp 783–788
23. Pinyi R, Yichen W, Qinghe D (2014) CAD-MAC: a channel-aggregation diversity based MAC protocol for spectrum and energy efficient cognitive ad hoc networks. *IEEE J Sel Areas Commun* 32(2):237–250
24. Wenshan Y, Pinyi R, Fan L, Qinghe D (2013) Joint sensing and transmission for AF relay assisted PU transmission in cognitive radio networks. *IEEE J Sel Areas Commun* 31(11):2249–2261
25. Dan HU, Hong-Jia LI, Xiao-Dong XU et al (2012) Inter-femtocell interference coordination in 3D in-building scenario. *J China Univ Posts Telecommun* 19(2):36–42
26. Liu J, Sun S, Liu J et al (2015) Hypergraph-based intercell interference coordination for QoS guarantees in dense femtocell networks. In: IEEE 81st vehicular technology conference (VTC Spring)
27. Yaacoub E (2014) Radio resource management in integrated wired/wireless LTE femtocell networks. In: Wired/wireless internet communications. Springer International Publishing, pp 96–108
28. Man C, Guomei Z, Shihua Z, Guobing L, Gangming L (2015) Interference coordination based on partial frequency band random allocation in LTE-advanced HetNet for internet of things. In: IEEE international conference on identification, information, and knowledge in the internet of things, pp 152–157
29. Wang J, Liu J, Wang D et al (2011) Optimized fairness cell selection for 3GPP LTE-A macro-pico HetNets. In: IEEE Vehicular Technology Conference, vol 16, no 2261, pp 1–5
30. Okasaka S, Yuda Y, Hoshino M (2013) An interference coordination method based on geometric mean of user throughput for heterogeneous networks. In: IEEE 24th international symposium on personal, indoor and mobile radio communications (Workshops), pp 179–183
31. 3rd Generation Partnership Project (3GPP) (2014) 3GPP TS 36.213 3GPP TSG RAN evolved universal terrestrial radio access (E-UTRA) physical layer procedures, version 12.2.0, Release 12
32. Qualcomm Inc (2013) 3GPP TSG-RANWG1 72 R1-130598, Agenda item: 7.3.7. Channel models for D2D deployments. St. Julians, Malta
33. Kennedy J, Eberhart R (1995) Particle swarm optimization. In: Proceedings of IEEE international conference on neural networks, pp 1942–1948